~~PNC TJ206 70-01 T~~

TJ206 71-11 T

~~PNC TJ206 71-11 T~~

Study of Heterogeneity Effects on the Sodium Void Coefficients (II)

August 1971

Mitsubishi Atomic Power Industries, Inc.

Study of Heterogeneity Effects on the Sodium Void Coefficient (II)

Abstracts

As a continuation of the previous research, heterogeneity effects of neutron spectra and axial leakage have been examined.

Spectra in a two-region cell were computed by a collision probability method and the heterogeneity effect was found to be small.

The analysis of the axial leakage was carried out with the Benoist's directional collision probability method and it turned out that the heterogeneity has negative contribution to the sodium void coefficient.

Combining the results of the previous research and the current one, the heterogeneous void coefficient in a prototype fast reactor moves towards the positive direction from the homogeneous result.

August, 1971

Takatoshi Kobayashi, Akira Sugawara

Yuji Seki, Yumiko Aoki

The work performed under contracts between Power Reactor and Nuclear Fuel Development Corporation and Mitsubishi Atomic Power Industries, Inc.

Study of Heterogeneity Effects on the Sodium Void Coefficient (II)

Contents

List of figures

List of tables

1. Introduction

In the core design of the fast neutron reactor sodium void coefficients are approximately calculated by homogenizing the fuel pin and coolant. As is well known, void coefficient consists of positive component due to spectral hardening and decrease of neutron absorption rate in sodium and negative component of increase in neutron leakage and therefore it is necessary to make a study, taking into consideration the heterogeneity effects on such factors. In the previous study, we formulated the collision probability method based on the integral transport theory to examine the heterogeneity effects on the neutron leakage by one group approximation.(1) Specifically, taking the core of a prototype reactor as the subject of our study, we exactly calculated the collision probability for the hexagonal lattice consisting of fuel pin and coolant to obtain the effective multiplication factors in normal and void conditions of the finite heterogeneous system with blanket. The same procedures applied to the homogenous system to examine the heterogeneity effects on the void coefficient. For axial leakage, we considered the form of DBz^2 by using the paste parameter of P_1 approximation.

In the present work the heterogeneity effect has been analyzed into spectrum components and axial leakage and investigated mainly by the collision probability method. As for the spectrum components, the neutron flux have been obtained in unit cell consisting of fuel pin and coolant from the 26-group collision probabilities, The same calculations applied to the homogeneous cell and examined thus obtained results, which are reported in Chapter 2. In Chapter 3, Benoist's directional collision probability(2) have been calculated with regard to the axial leaking. $DzBz^2$ in the heterogeneous system and homogeneous system have been evaluated by taking account of the anisotropy of the diffusion coefficient D. The previous approach has been used thereafter. Finally, all such results were reviewed in Chapter 4.

2. Spectrum effect

2.1 Formulation

In order to make comparison of spectrum between homogeneous and heterogeneous system, we approximated the reactor by a unit lattice consisting of two regions, fuel pin and coolant, and formulated it to obtain the multigroupe neutron flux in fuel pin and coolant by the collision probability method. The unit cell of hexagonal lattice was substituted by an equivalent cylindrical cell (Fig. 2.1)

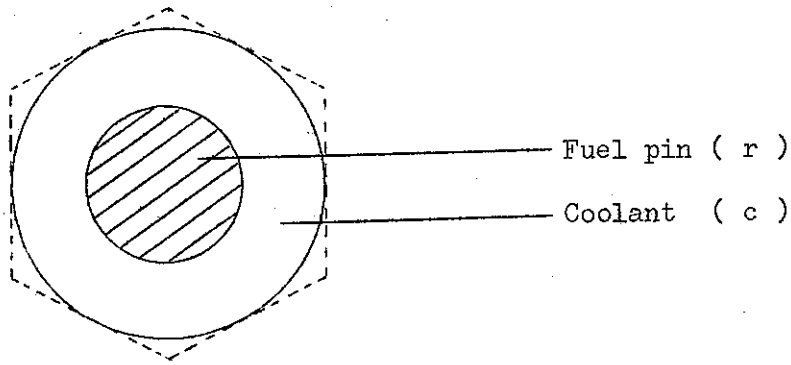

Fig. 2.1 Unit cell

If the probability that the neutrons emitted from a uniform and isotropic neutron source in the region α make a collisions in the region β is represented by $P_{\alpha\beta}$ and if a subscript r is used for the fuel pin region and C for the coolant region, we obtain the following balance equations.

$$\left.\begin{aligned} V_r \Sigma^i_{t,r} \phi^i_r &= V_r P^i_{rr} G^i_r + V_c P^i_{cr} G^i_c \\ V_c \Sigma^i_{t,c} \phi^i_c &= V_r P^i_{rc} G^i_r + V_c P^i_{cc} G^i_c \end{aligned}\right\} \quad (2.1)$$

where i represents energy group, V the volume of region, t the total cross section, and G and S are

$$\left.\begin{aligned} G^i_r &= \frac{1}{\lambda} X^i S_r + \mathrm{Sum}_k \Sigma^{k\to i}_r \phi^k_r \\ G^i_c &= \frac{1}{\lambda} X^i S_c + \mathrm{Sum}_k \Sigma^{k\to i}_c \phi^k_c \end{aligned}\right\} \quad (2.2)$$

$$\left.\begin{aligned} S_r &= \mathrm{Sum}_k\, \nu \Sigma^k_{f,r} \phi^k_r \\ S_c &= \mathrm{Sum}_k\, \nu \Sigma^k_{f,c} \phi^k_c \end{aligned}\right\} \quad (2.3)$$

when there is no upscatter, these equations can be further transformed for the convenience of numerical solution to

$$\left.\begin{aligned} & V_r (\Sigma^i_{t,r} - P^i_{rr} \Sigma^{i\to i}_r) \phi^i_r - V_c P^i_{cr} \phi^{i\to i}_c = S1 \\ & V_r P^i_{rc} \phi^i_r \Sigma^{i\to i}_r + V_c (\Sigma^i_{t,c} - (P^i_{cc} \Sigma^{i\to i})) \phi^i_c = S2 \end{aligned}\right\} \quad (2.4)$$

$$\left.\begin{aligned} S1 &= V_r P^i_{rr} \bar{G}^i_r + V_c P^i_{cr} \bar{G}^i_c \\ S2 &= V_r P^i_{rc} \bar{G}^i_r + V_c P^i_{cc} \bar{G}^i_c \end{aligned}\right\} \quad (2.5)$$

$$\left.\begin{aligned} \bar{G}^i_r &= \frac{1}{\lambda} X_i S_r + \mathrm{Sum}^{i-1}_{k=1} \Sigma^{k\to i}_r \phi^k_r \\ \bar{G}^i_c &= \frac{1}{\lambda} X_i S_c + \mathrm{Sum}^{i-1}_{k=1} \Sigma^{k\to i}_c \phi^k_c \end{aligned}\right\} \quad (2.6)$$

As in solving an ordinary diffusion equation, sources Sr and Sc are assumed initially and ϕ^i_r and ϕ^i_c are obtained one by one starting from the highest energy, i = 1 and recalculate the sources after the final group equation has been solved and the converged eigenvalue and ϕ^i_r and ϕ^i_c can be obtained by iteration method.

Prr, Prc, Pcr and Pcc in unit cell can be calculated by the following method. The probability when the cell in Fig. 2.1 is encircled by perfect black body is denoted by P^{bl}_{ij}, and if "white boundary condition"[3] (isotropic reflection condition) is assumed for the cell in the infinite lattice system, the probability Pij will be

$$\Sigma_i V_i P_{ij} = \Sigma_i V_i P^{bl}_{ij} + \frac{R_i R_i}{\mathrm{Sum} R_k} \quad (2.7)$$

$$R_k = \Sigma_k V_k (1 - \mathrm{Sum}_j P^{bl}_k) \quad (2.8)$$

P^{bl}_{ij} can be calculated exactly by Carlvik's method, as already shown in the previous report.

In the above equations, the finiteness of the system can be considered as an imaginary absorption in the form of DB^2.

2.2 Results of calculations

In order to examine the present analysis quantitatively, the prototype fast breeder system has been selected as an example.

The following assumptions have been made to facilitate the analysis.

i) Reactor has single region core, whose composition corresponds roughly to the average of actual inner and outer regions.

ii) Unit cell consists of two subregions; fuel region and coolant region.

iii) The fuel region is composed of fuel pellets and the coolant region is made of homogeneous mixture of fuel cladding material and sodium.

The fuel region is 0.275cm in radius and the equivalent cell radius is 0.41478 cm. At the computations, we used the modified ABN set and the self-shielding factors corresponding to the cell homogenized atom number densities at the normal and void condition, respectively. The axial reakage is included by an imaginary absorption DB^2 and also calculations were made by altering B^2.

As for buckling, three cases have been considered, where $B^2 = 1{,}608 \times 10^{-3}$ cm^{-2} corresponding to height of 90cm and core radius of 58.6cm, $B^2 = 0.0$, a perfect infinite lattice, and a set of bucklings for normal condition and void condition (B^2 normal $= 1{,}656 \times 10^{-3}$, B^2 void $= 1{,}460 \times 10^{-3}$). We obtained Pij from P_{ij}^{bl} for heterogeneous system and homogeneous system, respectively, and solved the equation (2.4) to obtain the eigenvalue and spectrum. Table 2.2 shows the results of calculations for the effective multiplication factor. Table 2.3 shows the constants contracted into one group by the neutron spectrum obtained in each case. In the case of heterogeneous system, the homogenized constants obtained from the contracted constants of fuel pin and coolant by volume-weighted-average are shown in the table for the convenience of comparison with the contracted constants by the spectrum obtained by making homogeneous calculation from the beginning.

Table 2.4 and Table 2.5 show the spectra when $B^2 = 1{,}608 \times 10^{-3}$, Fig. 2.2 and Fig. 2.3 show the their plots. In the homogeneous system, the spectra in fuel and coolant are naturally identical.

From these results it is seen that the heterogeneous Keff is higher than the homogeneous one both at normal and void conditions, which agreed with the general trend that the heterogeneous systems are more reactive than the homogeneous systems. The void coefficient becomes purely spectrum effect in a no leakage system where $B^2 = 0.0$ and only affects positively. The void coefficient becomes negative when leakage is taken into account in the form

of DB^2, where $B^2 = 1{,}608 \times 10^{-3}$ both for normal and void conditions and D is the cell-averaged value for each energy group corresponding to each condition. As is stated in Chapter 3, if it is set so that the total leakages may be equal both for normal and void conditions, the buckling itself changes somewhat. So, if the buckling is so taken as shown in Table 2.2, the void coefficient will become positive. However, no significant difference is observed in the value of void coefficient between the heterogeneous system and the homogeneous system. This is considered due to the fact that there is little difference in spectrum between the fuel and the coolant of the heterogeneous system. This is seen also from the fact that what is obtained by multiplying the one-groups coefficients of fuel and coolant of the heterogeneous system as shown in Table 2.2 by volume ratio and average virtually agrees with the constants of the homogeneous system. Therefore, from the cell calculations of 26 groups, it can be concluded that the heterogeneity effect of the spectrum is small.

3. Heterogeneity effects of axial leakage

When sodium void occurs in the heterogeneous system consisting of fuel pin and coolant, the neutron leakage increased along the voided channel and therefore it is considered that the axial leakage in the heterogeneous system causes negative on the void coefficient as compared with the homogeneous system. Here, taking into consideration the anisotropy of the lattice, the axial diffusion coefficient Dz was obtained by the Benoist's method, which, in the form of $DzBz^2$, was put into the neutron balance equation obtained by the collision probability method in the previous study and the heterogeneity effects on the void coefficient was examined quantitatively.

3.1 Method of calculating the axial diffusion coefficient Dz

As for the method of calculating the diffusion coefficient in the heterogeneous system, Benoist's[2] method is well known. This is a method in which the mean free path of each medium of the heterogeneous system is averaged by using the directional collision probability. The diffusion coefficient Dk is

$$DK=\frac{1}{3}\frac{\underset{i}{\mathrm{Sum}}\ \phi_i\ V_i\ \underset{i}{\mathrm{Sum}}\ \lambda_j\ P_{ijk}}{\underset{i}{\mathrm{Sum}}\ \phi_i\ V_i} \qquad (3.1)$$

$$P_{ijk}=\iiint_{Ri}\frac{dr_1}{Vi}\iiint_{Ri}\frac{dr_2\cdot\Sigma_j}{4\pi|r_2-r_1|^2}\cdot 3\Omega^2_k \qquad (3.2)$$

where k represents direction, ϕ i and Vi represent the mean neutron flux and the region volume in the i region, respectively, and Pijk represents the directional collision probability from the region i to the region j.

The axial diffusion coefficient Dz can be obtained by using $3\cos^2\Theta$ for $3\Omega^2_k$, in which Θ is the angle between by the direction of the neutron flight path and the Z axis.

Assuming uniformity in the axial direction, the probability, in the case of directional collision probability, that the neutrons generating from the linear source do not collide as far as the point where the projection on the plane XY is denoted by T is given by

$$Pz(T)=3[Ki_2(T)-Ki_4(T)] \qquad (3.3)$$

Therefore, the directional collision probability Pijz from the region i to the region j in Fig. 3.1 can be expressed by the following equation.

$$P_{ijkz}=\frac{2}{2\pi\Sigma_i V_i}\int d\Psi\int dy\,[Ki_3(Tij)-Ki_3(Ti+Tij)$$
$$-Ki_3(Tij+Tj)+Ki_3(Ti+Tij+Tj)$$
$$-Ki_5(Tij)+Ki_5(Ti+Tij)$$
$$+Ki_5(Tij+Tj)-Ki_5(Ti+Tij+Tj) \qquad (3.4)$$

and similary

$$P_{ijz}=1-\frac{3}{2\pi\Sigma_i V_i}\int d\Psi\int dy\,[Ki_3(0)-Ki_3(Ti)$$
$$-Ki_5(0)+Ki_5(Ti)] \qquad (3.5)$$

The collision probability in the hexagonal lattice consisting of fuel pin and coolant region is approximated by the collision probability in the cylindrical cell on which the isotropic reflection condition is imposed.

The fuel is expressed by subscript r and the coolant by c. In order to obtain the directional collision probabilities P^1_{rrz}, P^1_{rcz}, P^1_{crz} and P^1_{ccz} in the isolated cylindrical two-region cell, we took the neutron flight path perpendicular to the radius at the respective points on one radius and performed the numerical integration of the above equation. Since cylindrical shape is assumed, there is no need for the integration of $\int d\Psi$ from symmetry. Here, P^1_{rcz} means the probability that the neutrons starting from the fuel make the first collision in the coolant without reaching the cell boundary and the same also applies to others. These correspond to P^{bl}_{rc} and others in the preceding paragraph. These collision probabilities were obtained numerically by using the computer code CPROP for the collision probability of concentric cylindrical multiregion system. (See Appendix)
The one group constants, fuel rod radius, equivalent radius of coolant of sample calculation are fabulated in Table 3.1.

$$D_{homog}=\frac{1}{3\Sigma}\ ,\quad .\quad \Sigma=(\Sigma_r V_r+\Sigma_c V_c)/(V_r+V_c)$$

The directional collision probabilities Prrz, Prcz, Pcrz and Pccz in the cylindrical cell on which the isotropic reflection condition is imposed can be easily obtained by using the above collision probabilities in the isolated cell. (See Section 2.) These directional collision probabilities at normal and void conditions and collision probabilities are shown in Table 3.2 and Table 3.3.

The calculation of diffusion coefficients further requires the average neutron flux in each region. Assuming an infinite system without leakage, we obtained the same values of 1.0002 for the fuel-to-coolant mean neutron flux ratio $\Phi f/\Phi c$ both in normal and void condition by the neutron balance by collision probability.

The axial diffusion coefficients obtained by the equation (3.1) are given in Table 3.4. The diffusion coefficients of homogeneous system Dhomog in this table are given by the following formula, using the volume-weighted-average of the transport cross sections.

The mean value $\overline{D}$ of heterogeneous system corresponds to the case where the system is not anisotropic and was obtained by the equation (3.1) by using collision probability instead of directional collision probability.

Between the homogeneous diffusion coefficient Dhomog and the heterogeneous diffusion coefficient Dz is observed a difference of 0.49% in normal condition and 1.38% in void condition.

3.2 Calculation of void coefficient

Next, it is necessary to denote the axial leakage by the equivalent absorption DB^2. Usually, the axial buckling Bz^2 decreases as the diffusion coefficient of the core increases and therefore we calculated Bz^2 by buckling search both in normal and void condition. The core and blanket were similar with those given in Table 3.1. Of the core constants, we used the heterogeneous average $\overline{D}$ (Table 3.3) for the diffusion coefficient and homogeneous coefficients (Table 3.1) for other constants.

The buckling search was done, following the procedure below.

(1) One-dimentional radial distribution of neutron flux is calculated with B_z^2 being changed parametrically and B_r^2 at the respective Bz^2 is calculated from the neutron leakage at the boundary of core and radial blanket.

(2) In the calculation of one-dimentional axial distribution of neutrons, Bz^2 at the respective Br^2 is calculated from the neutron leakage at the boundary between core and axial blanket by changing Br^2 in a similar manner.

(3) A Br^2 Vz Bz^2 graph is drawn and Bz^2 is obtained from the intersection of (1) and (2). The result is shown in Fig. 3.2.

From this it is shown that the value of buckling calculated from the neutron leakage is little dependent upon the given value of the radial buckling.

The obtained values of axial buckling are shown in Table 3.5.

If the diffusion coefficient increases by +25.4% from 1.3749 in normal condition to 1.7123 in void condition, Bz^2 decreases by 11.71% from the results in Table 3.5 and the equivalent leakage DB^2 increases by +9.9%. In other words, it can be said that the increase in leakage amounts to only 0.4% in contrast to a 1% increase in diffusion coefficient.

The system's effective multiplication factor keff was calculated by adding the term of the axial leakage of DB^2 to the neutron balance equation by collision probability in the previous work.

For the calculation of DB^2, we used Bz^2 given in Table 3.5. We used the heterogeneous axial diffusion coefficient Dz for leakage in heterogeneous system and the diffusion coefficient in homogeneous condition Dhomog for leakage in homogeneous system and synthesized D x B^2. Using these DB^2, we repeated part of the analysis by the collision probability method in the previous research. For the collision probability method in heterogeneous system, we made two kinds of calculation using heterogeneous $DzBz^2$ and homogeneous Dhomog B^2, respectively, while for homogeneous system, making only one kind of calculation, using the homogeneous Dhomog, to obtain the effective multiplication factor. The results of calculations are shown in Table 3.6.

In this collision probability method we used the Method B which was described in the previous work (a method based on the Bonalumi's assumption that the angular distribution is uniform for the neutron flux passing through the boundary between core and blanket.

4. Conclusion

In this chapter we will make an overall review of the subjects which were discussed separately in the preceding Chapter 2 and 3. As was discussed in Chapter 2, no significent difference between homogeneous system and heterogeneous system has been found in one-group constants obtained from multi-group spectrum of a typical cell. Therefore, it seems to be allowable that, as was done in the previous work and Chapter 3 of this paper, the values obtained by multiplying the one-group constants of fuel pin and coolant of the heterogeneous system by volume ratio and averaging them are used as the constants of the homogenous system in the analyses.

Next, let us consider the heterogeneity effects of axial leakage on the void coefficients. The difference, kvoid (kvoid - knormal), between keff in void condition and keff in normal condition is called the "void coefficient". Comparing the results of two calculations by the heterogeneous collision probability method from Table 3.6, it is shown that a negative effect of 0.0009 is caused by heterogeneity of diffusion coefficient on kvoid. In the case of the fast reactor, the neutron leakage from the core is so large that the effective multiplication factor is sensitive to the diffusion coefficient of the system. The difference 1.1% between the change 23.78% of the homogeneous diffusion coefficient from void condition to normal condition and the change 24.89% of the heterogeneous axial diffusion coefficient Dz has brought about a difference of 0.0009 to kvoid. This result is understandable also from the magnitude of constribution of L^2 B^2 in the point model equation, keff = k $/(1 + L^2B^2)$. As was mentioned in the Section 3.2, for making DB^2 which was used in this calculation, we used the same value of axial buckling both for homogeneous and heterogeneous systems and used different values for the diffusion coefficient D, that is, we used Dhomog for homogeneous system and Dz for heterogeneous system. However, considering the buckling Bz^2 decreases as Dz increases in heterogeneous system, the difference of DB^2 between heterogeneous and homogeneous systems becomes further smaller. Therefore, the difference 0.0009 of kvoid obtained here is a quantity which is considered to be reasonable as the maximum value of the axial heterogeneity effect.

On the other hand there remains a difference of 0.0068 between kvoid (= -0.0168) obtained by the collision probability in heterogeneous system and kvoid (= -0.0236) obtained by the collision probability in homogeneous

system almost as in the previous work and the homogeneous system has more negative effect. This tendency was discueed in the previous work. If the probability that the neutrons generating in the fuel region leak out of cell in the heterogeneous system compares with that in the homogeneous system, the leakage obtained by using the collision probability in Table 3.2 is 0.8589 in the heterogeneous system and 0.8700 in the homogeneous system, that is, the homogeneous system has greater probability that the neutrons excape out of cell. On the other hand, the probability that the neutrons generating in the coolant region leak out of cell is 0.9011 in the heterogeneous system and 0.8954 in the homogeneous system, showing a reverse tendency. However, since the fuel region has far higher rate of secondary neutron generation in the heterogeneous system, the probability that secondary neutrons generating in cell escape the cell is 0.8754 in the heterogeneous system and 0.8842 in the homogeneous system, that is, the value is greater in the homogeneous system. This fact qualitatively confirms that the value of void coefficient has more negative tendency in the homogeneous system than in the heterogeneous system.

From what we have just discussed, it can be concluded that when there has occurred 100% loss of sodium in the core in the prototype reactor, the effect on axial leakage will be negative in the heterogeneous treatment but the total void coefficient shows more positive value as compared with the value in the homogeneous system.

Bibliography

(1) Study of heterogeneity effects on sodium void coefficient
(The work performed under contracts with the Power Reactor and Nuclear Fuel Development Corporation (PNC), SJ 206 70-01)

(2) P. Benoist, Théorie du coefficient des diffusion des neutrons dans un réseau comportant des cavités, CEA-R2278

(3) I. Carlvik. A method for calculating collision probabilities in general cylindrical geometry and applications to flux distributions and Dancoff factors, proc. 3rd Geneva Conf. P/681 (1964)

Appendix Explanations on computer codes

Explanations on the calculation codes used in the present work are given in (1) and (2) and the mutual relations between the computer codes are explained in (3). The computer used in the present study is IBM360/75J and all programs used on this computer are written in Fortran IV.

(1) Cell spectrum calculation code

This code calculates neutron flux in cell and eigenvalue. All input data are prepared by the namelist format and the following are required.

(i) Input apparatus No. 5

TITLE (20) FORMAT (20A4)

& INPUT

V(1) = fuel pin volume, coolant volume

CHI(1) = fission spectrum (from group 1 to 26)

EPS = convergence criteria of eigenvalue

& END

(ii) Input apparatus No. 8

Comment Card		80X
Prr Prc	Group 1	2E12.5
Pcr Pcc		2E12.5
Comment Card		80X
Prr Prc	Group 2	2E12.5
Pcr Pcc		2E12.5
⋮	⋮	
	Group 26	

(iii) Input apparatus No. 9

& OUTPUT

SIGTB (1 , 1) = $(\Sigma t + DB^2)_r$ from Group 1 to 26,

SIGTB (1 , 2) = $(\Sigma t + DB^2)_c$ from Group 1 to 26,

SIGTR (1 , 1) = Σt, r from Group 1 to 26,

SIGTR (1 , 2) = Σt, c from Group 1 to 26,

SIGKI (1 , 1 , 1) = $\Sigma_r^{i \to j}$ assignment varying i with fixed j, both in ascending order

SIGKI (1 , 1 , 2) = $\Sigma_c^{i \to j}$ assignment varying i with fixed j, both in ascending order.

SIGNF (1 , 1) = $\nu \Sigma f$, r(from Group 1 to 26),

SIGNF (1 , 2) = $\nu \Sigma f$, c(from Group 1 to 26),

SIGA (1 , 1) = Σa, r(from Group 1 to 26),

SIGA (1 , 2) = Σa, c(from Group 1 to 26),

& END

(iv) Output

Eigenvalue, neutron flux, one group contracted coefficient

(2) Collision probability of concentric cylindrical multiregion system and directional collision probability calculation code "CPROP"

The collision probability Pij in the concentric cylindrical region can be estimated by drawing the neutron flight path in Carlvik's method. The integration of collision probability of each neutron path is performed by using the trapezoidal integration formula. The Ki_3 function have been estimated by the accurate approximate function formula which was described in the previous report. The directional collision probability Pijz is also obtained by similar method. Ki_5 function is obtained by direct numerical integration.

(i) Input data

TITLE (20) FORMAT (20A4)

& INPUT

ITYPE = 0/1 first collision probability/ directional collision probability

NREG = Number of regions ($\leq$ 50)

NP(i) = Number of neutron flight path in the regions of thickness in each region

RAD(i) = Outer radius (cm) of each region

SIG(i) = Total cross section (cm -1) of each region

& END

(ii) Output data

P^1 ij or P^1 ijz list

(3) List of codes used in the analysis of void coefficient heterogeneity

Here, the mutual relations between the computer codes used in the present and previous study are explained. For detailed contents of calculations, refer to the previous report.

(i) FFCP: To calculate exactly the collision probability from cell to cell in the hexagonal lattice.

(ii) Distant-FFCP: To homogenize the internediate medium and make approximate calculation of collision probability between distant cells.

(iii) Zone-to-Zone: To convert the cell-to-cell collision probability into the zone-to-zone probability by averaging.

(iv) Distant Zone-to-Zone: To obtain the zone-to-zone probability between distant zones on the basis of (ii).

(v) Homog Cylinder: To calculate the collision probability from ring to ring in the concentric cylindrical region. This resembles CPROP but has an option of the black body center.

(vi) MERGE 2: To combine the collision probability in the core, which was calculated in (iii) and (iv) with the probability of (v) by the Method $A^{(1)}$ and make probability including the blanket region.

(vii) MERGE 3: To use Method $B^{(1)}$ to do the same as above (vi).

(viii) EIGEN: To calculate the effective multiplication factor for a reactor by using the probability made by MERGE2 or MERGE3.

The relations of the above codes and those which were used in the present investigation are diagramatically shown in Fig. A-1.

Table 2.1 Atom number density (x $10^{24}/cm^3$)

	Fuel pin	Coolant region	Homogenized atomic number density
O	4.201 - 2	0.0	1,8466 - 2
Na	0.0	1.415 - 2 (0.0)	7.9300 - 3 (0.0)
Cr	0.0	4.895 - 3	2.7432 - 3
Fe	0.0	1.842 - 2	1.0323 - 2
Ni	0.0	2.447 - 3	1.3713 - 3
U235	2.362 - 5	0.0	1.0382 - 5
U236	1.732 - 6	0.0	7,6133 - 7
U238	1.528 - 2	0.0	6.7166 - 3
Pu239	3.149 - 3	0.0	1.3842 - 3
Pu240	1.262 - 3	0.0	5.5473 - 4
Pu241	2.457 - 4	0.0	1.0800 - 4
Pu242	1.262 - 5	0.0	5.5473 - 6
FP.U	1.038 - 4	0.0	4.5627 - 5
FP.Pu	9.141 - 4	0.0	4.0181 - 4
Volume ratio in unit cell	0.43957	0.56043	

Table 2.2 Results of cell calculations

		B^2 cm^{-2}	Keff	k_{void} ($=k_{void}-k_{normal}$)
Heterogeneous	Normal	1.608 - 3	1.11268	-0.02372
	Void	1.608 - 3	1.08896	
Homogeneous	Normal	1.608 - 3	1.111151	-0.02375
	Void	1.608 - 3	1.08776	
Heterogeneous	Normal	0.0	1.47279	+0.05946
	Void	0.0	1.53225	
Homogeneous	Normal	0.0	1.47149	+0.005911
	Void	0.0	1.53060	
Heterogeneous	Normal	1.6555 - 3	1.10438	+0.01534
	Void	1.4605 - 3	1.11972	
Homogeneous	Normal	1.6555 - 3	1.10321	+0.01529
	Void	1.4605 - 3	1.11850	

Table 2.3 Comparison of one-group contracted coefficients in cell calculation

	B^2 cm^{-2}	$\Sigma_{tr} + DB^2 cm^{-1}$	$\upsilon\Sigma_f$ cm^{-1}	Σ_a cm^{-1}
Heterogeneous, normal, fuel	1.608 x 10^{-3}	0.33578	0.022385	0.014116
Coolant		0.15317	0.0	0.00022678
Volume average		0.233440	0.0098398	0.0063321
Homogeneous, normal, fuel equivalent		0.23340	0.0098360	0.0063307
Coolant equivalent		0.23340	0.0098361	0.0063307
Coolant equivalent		0.32912	0.022069	0.01324
Heterogeneous, void, fuel		0.091784	0.0	0.00019260
Coolant		0.196110	0.0097009	0.0059278
Volume average		0.19608	0.0096986	0.0059263
Homogeneous, void, fuel equivalent		0.19608	0.0096987	0.0059263
Coolant		0.19608	0.0096987	0.0059263
Heterogeneous, normal, fuel	0.0	0.34346	0.022136	0.014814
Coolant		0.15806	0.0	0.00023525
Volume average		0.239556	0.0097303	0.0066436
Homogeneous, normal, fuel equivalent		0.23950	0.0097275	0.0066415
Coolant equivalent		0.23950	0.0097276	0.0066415
Heterogeneous, void, fuel		0.33882	0.021531	0.013888
Coolant		0.094294	0.0	0.00019634
Volume average		0.201780	0.0094644	0.0062148
Homogeneous, void, fuel equivalent		0.20174	0.0094632	0.0062128
Coolant equivalent		0.20174	0.0094633	0.0062128

Table 2.4 Neutron flux in cell (B^2=1,608x10^{-3}cm^{-2})
(Heterogeneous)

	Heterogeneous (normal)		Heterogeneous (void)	
Energy group	Fuel pin	Coolant	Fuel pin	Coolant
6.5 -10.5 Mev	4.175- 1	4.109+ 1	4.536- 1	4.479- 1
4.0 - 6.5	2.639	2.602	2.857	2.825
2.5 - 4.0	6.279	6.215	6.703	6.648
1.4 - 2.5	1.292+ 1	1.285+ 1	1.352+ 1	1.346+ 1
0.8 - 1.4	1.698+ 1	1.696+ 1	1.821+ 1	1.821+ 1
0.4 - 0.8	3.224+ 1	3.222+ 1	3.556+ 1	3.557+ 1
0.2 - 0.4	3.440+ 1	3.441+ 1	3.523+ 1	3.524+ 1
0.1 - 0.2	3.406+ 1	3.404+ 1	3.396+ 1	3.393+ 1
46.5 -100 kev	2.750+ 1	2.749+ 1	2.681+ 1	2.680+ 1
21.5 -46.5	1.901+ 1	1.903+ 1	1.681+ 1	1.682+ 1
10.0 -21.5	1.169+ 1	1.171+ 1	9.617	9.627
4.65 -10.0	5.691	5.691	4.365	4.364
2.15 - 4.65	1.669	1.659	2.247	2.256
1.0 - 2.15	2.445	2.479	9.579- 1	9.609- 1
465 -1000 ev	9.309- 1	9.390- 1	2.938- 1	2.951- 1
215 -465	2.755- 1	2.785- 1	7.852- 2	7.916- 2
100 -215	6.478- 2	6.580- 2	1.676- 2	1.697- 2
46.5 -100	9.805- 3	1.009- 2	2.283- 3	2.336- 3
21.5 -46.5	1.867- 3	1.907- 3	3.945- 4	4.013- 4
10.0 -21.5	1.717- 4	1.805- 4	3.256- 5	3.390- 5
4.65-10.0	1.412- 5	1.497- 5	2.388- 6	2.504- 6
2.15- 4.65	4,116- 6	4.161- 6	6.311- 7	6.366- 7
1.0 - 2.15	2.227- 7	2.427- 7	3.047- 8	3.269- 8
0.465-1.0	8.405- 9	9.642- 9	1.007- 9	1.127- 9
0.215-0.465	6.820-11	1.293-10	7.052-12	1.223-11
0.0252	1.105-12	1.913-12	9.130-14	1.464-13

Table 2.5 Neutron flux in cell ($B^2 = 1.608 \times 10^{-3} cm^{-2}$)
(Homogeneous)

	Homogeneous (normal)		Homogeneous (void)	
Energy group	Fuel equivalent	Coolant equivalent	Fuel equivalent	Coolant equivalent
6.5 -10.5 Mev	4.149- 1	4.149- 1	4.517- 1	4.517- 1
4.0 - 6.5	2.624	2.624	2.846	2.846
2.5 - 4.0	6.255	6.255	6.685	6.685
1.4 - 2.5	1.290+ 1	1.290+ 1	1.350+ 1	1.350+ 1
0.8 - 1.4	1.698+ 1	1.698+ 1	1.821+ 1	1.821+ 1
0.4 - 0.8	3.224+ 1	3.224+ 1	3.556+ 1	3.556+ 1
0.2 - 0.4	3.440+ 1	3.440+ 1	3.522+ 1	3.522+ 1
0.1 - 0.2	3.404+ 1	3.404+ 1	3.393+ 1	3.393+ 1
46.5 -100 Kev	2.748+ 1	2.747+ 1	2.678+ 1	2.678+ 1
21.5 -46.5	1.900+ 1	1.900+ 1	1.679+ 1	1.679+ 1
10.0 -21.5	1.168+ 1	1.168+ 1	9.601	
4.65 -10.0	5.684	5.684	4.356	4.355
2.15 - 4.65	1.660	1.660	2.244	2.243
1.0 - 2.15	2.452	2.451	9.555- 1	9.554- 1
465 -1000 ev	9.289- 1	9.288- 1	2.929- 1	2.929- 1
215 -465	2.743- 1	2.743- 1	7.823- 2	7.822- 2
100 -215	6.432- 2	6.431- 2	1.667- 2	1.666- 2
46.5 -100	9.688- 3	9.687- 3	2.263- 3	2.263- 3
21.5 -46.5	1.826- 3	1.826- 3	3.883- 4	3.883- 4
10.0 -21.5	1.667- 4	1.667- 4	3.190- 5	3.190- 5
4.65 -10.0	1.346- 5	1.345- 5	2.310- 6	2.310- 6
22.15 - 4.65	3.829- 6	3.829- 6	6.008- 7	6.008- 7
1.0 - 2.15	2.069- 7	2.069- 7	2.898- 8	2.898- 8
0.465- 1.0	7.544- 9	7.543- 9	9.353-10	9.352-10
0.215- 0.465	5.785-11	5.785-11	6.308-12	6.307-12
0.0252	6.806-13	6.804-13	6.507-14	6.506-14

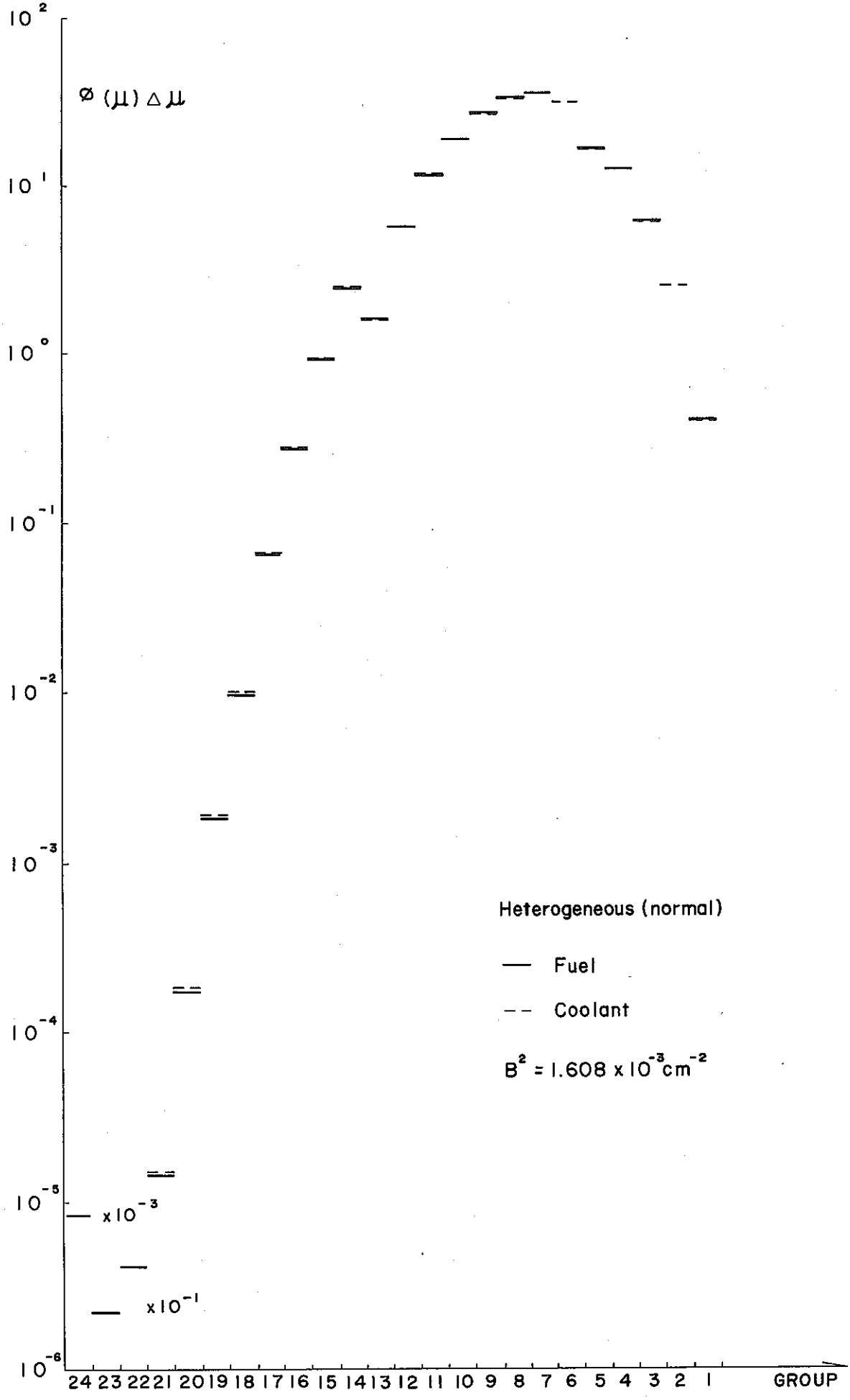

Fig. 2.2 Neutron spectrum

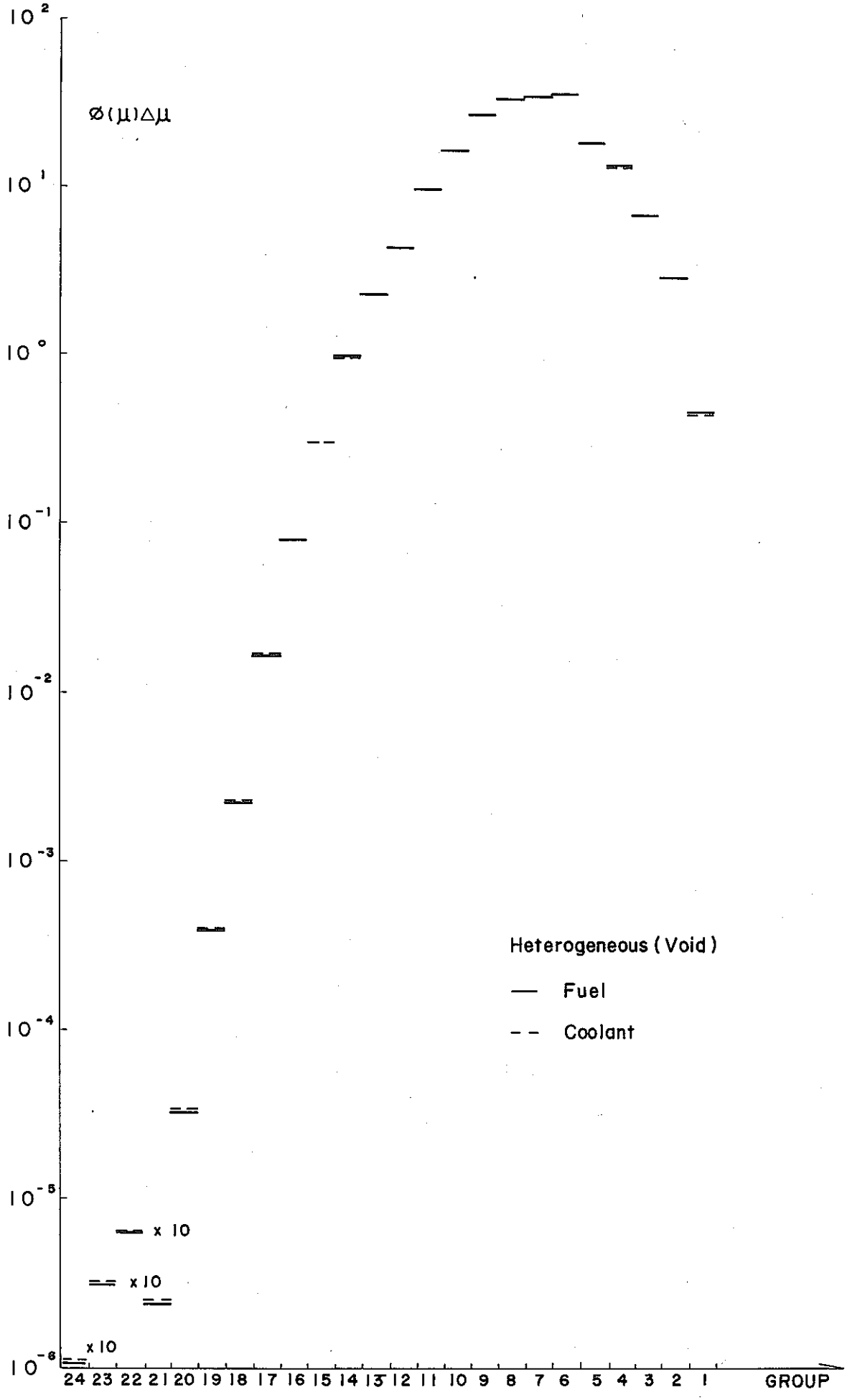

Fig. 2.3 Neutron spectrum

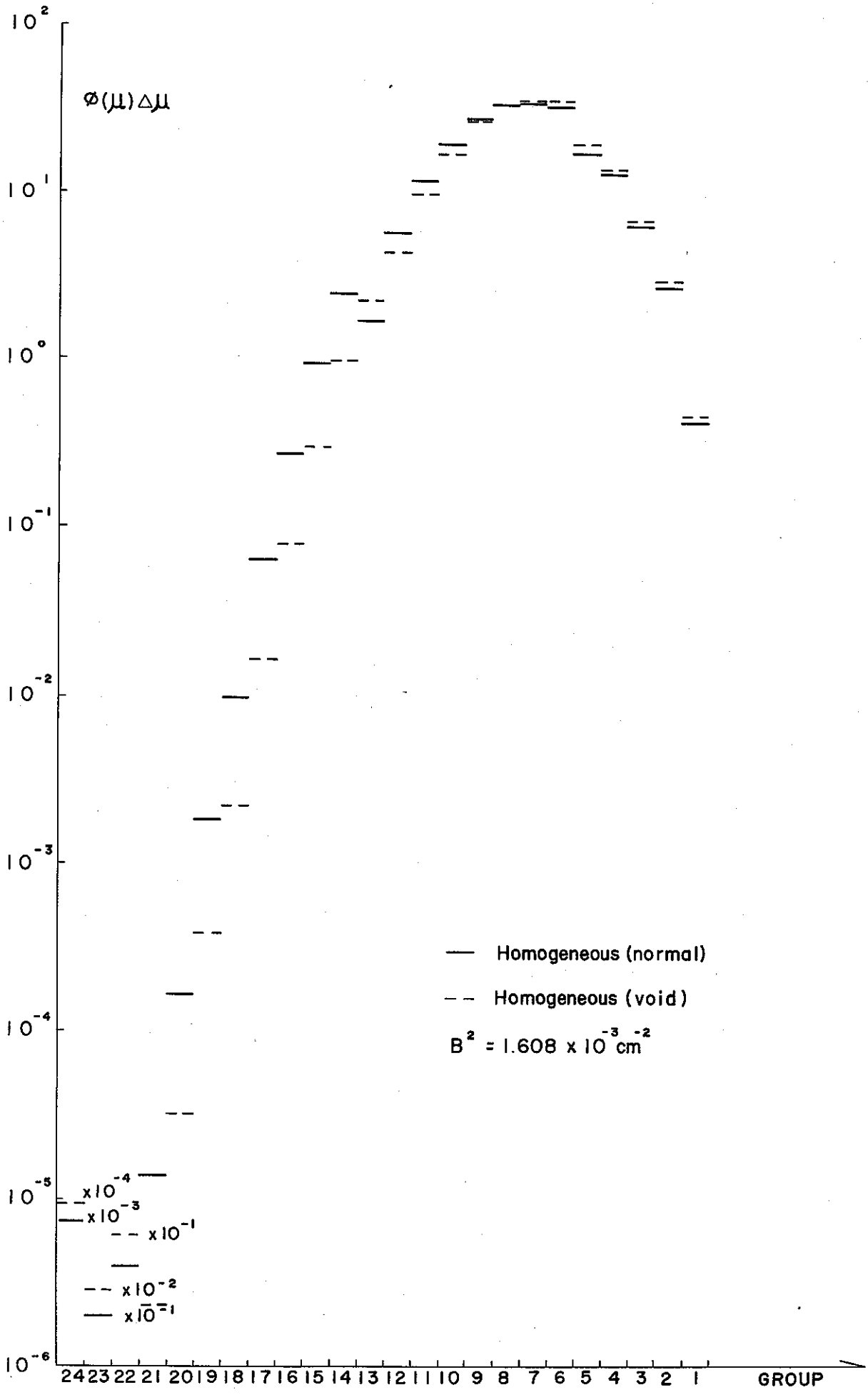

Fig. 2.4 Neutron spectrum

Table 3.1 Constants and specification

	Reactor core						Blanket
	Fuel rod		Cooland		Homogenization		
	Normal	Void	Normal	Void	Normal	Void	
t (cm^{-1})	0.3342	0.3342	0.1719	0.08852	0.24324	0.19651	0.30183
a (cm^{-1})	0.01473	0.01473	0.0006181	0.0005875	0.0068212	0.0068041	0.004966
f(cm^{-1})	0.02218	0.02218	0.0	0.0	0.0097497	0.0097497	0.001098

Fuel pin diameter	0.55	cm	Fuel volume ratio	0.43957	cm
Fuel pin pitch	0.79	"	Coolant volume ratio	0.56043	"
Equivalent cell radius	0.41478	"	Thickness of radial blanket	26.404	cm
Core radius	58.596	"			
Core height	90.0	"	Thickness of axial blanket	30.0	"

Table 3.2 Collision probability in isolated cell

	Normal	Void
Collision probability		
Prr^1	0.10677	0.10677
Prc^1	0.034293	0.017923
Pcr^1	0.052294	0.053474
Pcc^1	0.046570	0.024407
Directional collision probability		
$Prrz^1$	0.14817	0.14817
$Prcz^1$	0.045989	0.024227
$Pcrz^1$	0.070129	0.071743
$Pccz^1$	0.064744	0.034045

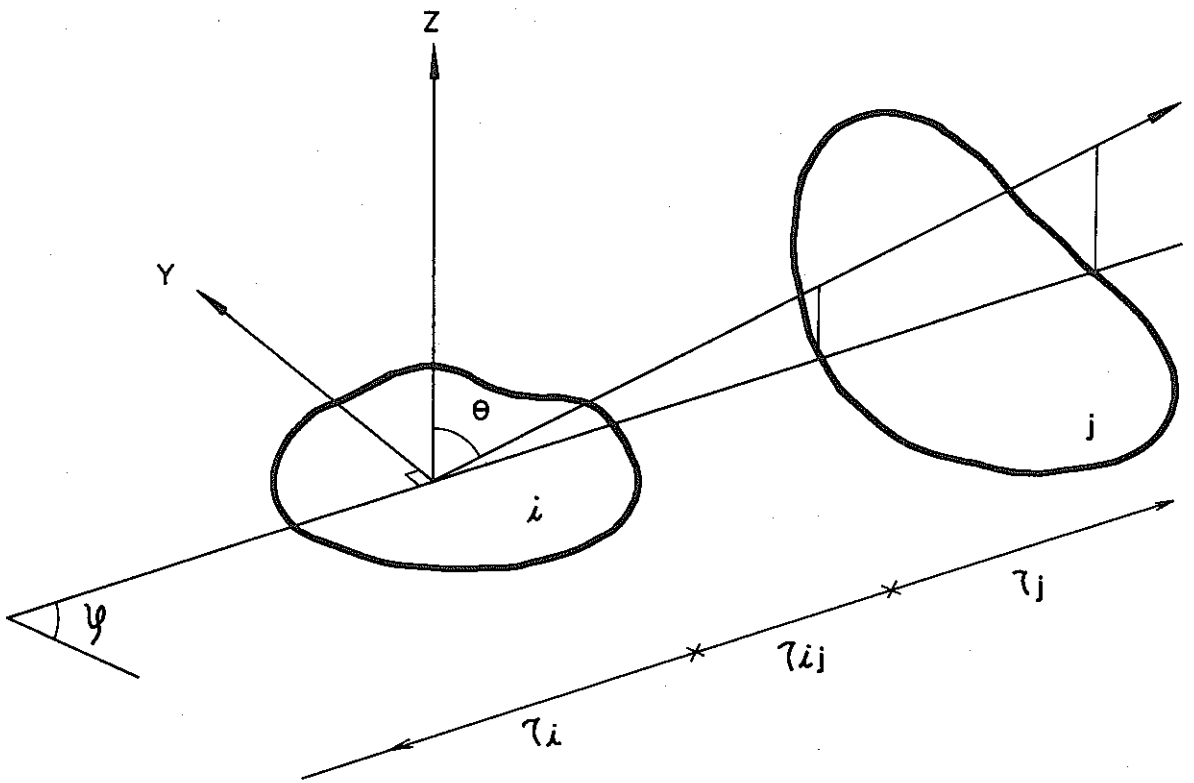

Fig. 3.1 Neutron flight path

Table 3.3 Collision probability in lattice cell

	Normal	Void
Collision probability		
Prr	0.61562	0.75232
Prc	0.38438	0.24768
Pcr	0.58614	0.73344
Pcc	0.41386	0.26656
Directional collision probability		
Prr	0.62107	0.75453
Prc	0.37893	0.24547
Pcr	0.57782	0.27310
Pcc	0.42218	0.72690

(Cylindrical approximation, isotropic reflection condition)

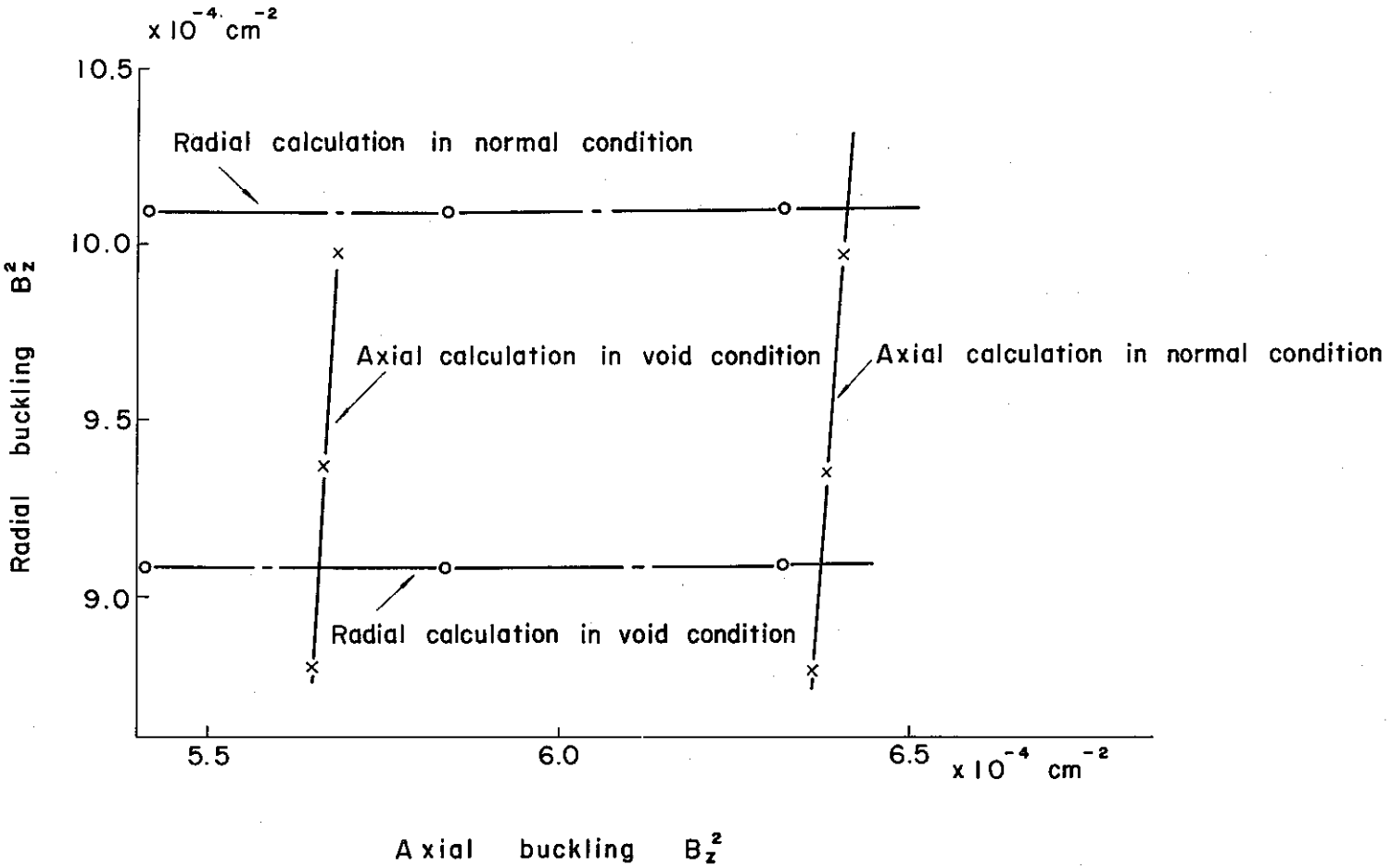

Fig. 3.2 Buckling search

Table 3.4 Diffusion coefficients

	Homogeneous	Heterogeneous		
	Dhomog	Dz (Axial)	Dr (Radial)	$\overline{D}$ (Average)
Normal	1.3704	1.37706	1.37387	1.37493
Void	1.6963	1.71975	1.70861	1.71232

Table 3.5 Axial buckling

	Normal	Void
B_z^2 (cm^{-2})	6.4066×10^{-4}	5.6564×10^{-4}

Table 3.6 Void coefficients

Collision probability method	Heterogeneous collision probability method		Homogeneous collision Probability method
Axial leakage	Heterogeneous Dz x Bz^2	Homogeneous Dhomog x Bz^2	Homogeneous Dhomog x Bz^2
Effective multiplication factor keff			
Normal	1.0476	1.0481	1.0465
Void	1.0299	1.0313	1.0229
Void coefficient			
kvoid	-0.0177	-0.0168	-0.0236

Void coefficient kvoid = keff (void) - keff (normal)

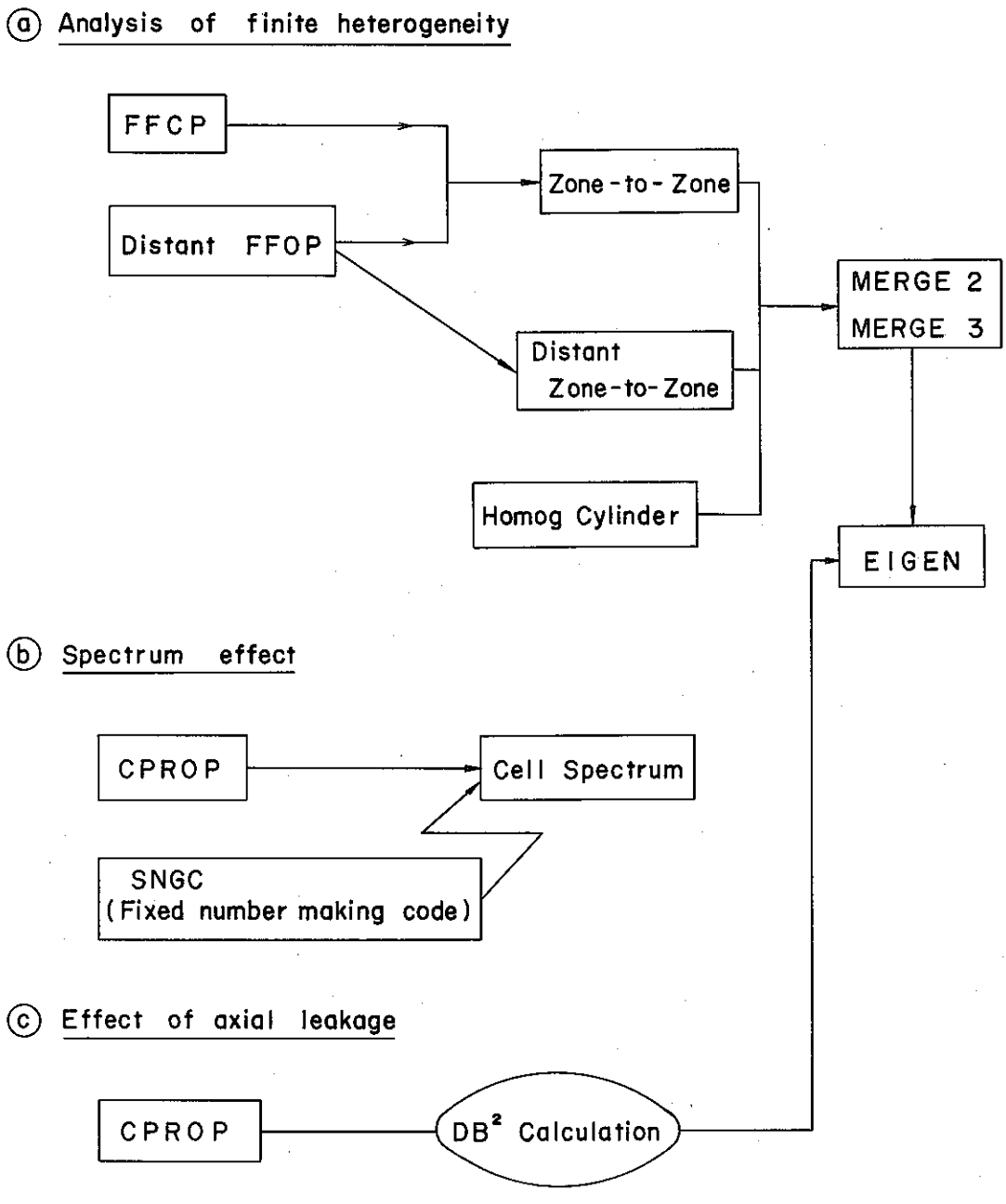

Fig. A-1 Block diagram of calculation code